AIP Applied Physics Letters

Antiferromagnetic coupling across silicon regulated by tunneling currents

R. R. Gareev, M. Schmid, J. Vancea, C. H. Back, R. Schreiber et al.

Citation: Appl. Phys. Lett. **100**, 022406 (2012); doi: 10.1063/1.3675872
View online: http://dx.doi.org/10.1063/1.3675872
View Table of Contents: http://apl.aip.org/resource/1/APPLAB/v100/i2
Published by the American Institute of Physics.

APPLIED PHYSICS LETTERS **100**, 022406 (2012)

Antiferromagnetic coupling across silicon regulated by tunneling currents

R. R. Gareev,[1,a)] M. Schmid,[1] J. Vancea,[1] C. H. Back,[1] R. Schreiber,[2] D. Bürgler,[2] C. M. Schneider,[2,3] F. Stromberg,[3] and H. Wende[3]
[1]*Institute of Experimental and Applied Physics, University of Regensburg, 93040 Regensburg, Germany*
[2]*Institute of Solid State Research (IFF), Research Center Juelich, 52428 Juelich, Germany*
[3]*Faculty of Physics and Center for Nanointegration Duisburg-Essen (CeNIDE), University of Duisburg-Essen, 47048 Duisburg, Germany*

(Received 18 May 2011; accepted 13 December 2011; published online 10 January 2012)

We report on the enhancement of antiferromagnetic coupling in epitaxial Fe/Si/Fe structures by voltage-driven spin-polarized tunneling currents. Using the ballistic electron magnetic microscopy, we established that the hot-electron collector current reflects magnetization alignment and the magnetocurrent exceeds 200% at room temperature. The saturation magnetic field for the collector current corresponding to the parallel alignment of magnetizations rises up with the tunneling current, thus demonstrating stabilization of the antiparallel alignment and increasing antiferromagnetic coupling. We connect the enhancement of antiferromagnetic coupling with local dynamic spin torques mediated by spin-polarized tunneling electrons. © *2012 American Institute of Physics*. [doi:10.1063/1.3675872]

Antiferromagnetic (AF) interlayer exchange coupling between magnetic layers separated by metallic or insulating spacers is a basic effect for spintronics.[1,2] It is well established that AF coupling across metals is accompanied by the giant magnetoresistance effect, where resistance depends on the relative alignment of magnetic electrodes due to spin-dependent interface scattering.[3] Ferromagnetic layers separated by a thin tunneling barrier (TB) demonstrate interlayer coupling mediated by spin-polarized conduction electrons via equilibrium spin-torques.[4,5] A possible way to regulate AF coupling across TB's[6–8] could be in utilization of dynamic spin-transfer torques produced by voltage-driven tunneling currents. Spin-polarized currents with sufficient current densities can influence total in-plane spin torques and, consequently, the strength of AF coupling.[9] This approach promises voltage-controlled AF coupling for spintronics devices.

Tunneling structures based on Si are attractive due to their compatibility with existing semiconductor technologies and prospective for spin-injection devices due to low spin-orbit scattering in this material.[10] Earlier we found strong AF coupling across Si TB's.[7] Theoretical modeling showed that resonant impurity states in a spacer layer can lead to specific tunneling magnetoresistance (TMR) and enhanced AF coupling.[11] In accordance, we confirmed the formation of a TB with a low resistance-area product[8] as well as resonant-type TMR in Si-based tunneling structures.[12] However, room-temperature (RT) spin-dependent magnetotransport in Fe/Si/Fe was not observed so far.

We prepared AF-coupled epitaxial Fe(3 nm)/Si(2.4 nm)/Fe(3 nm)/Au(6 nm) structures on a 7-μm-thick $Ga_{0.67}P_{0.33}As$ (100) layer ($n = 5*10^{16}\,cm^{-3}$) grown on a GaAs (100) ($n = 1*10^{18}\,cm^{-3}$) wafer using thermal electron-gun evaporation as described elsewhere.[7] Before evaporation, we performed annealing of the substrate at $T = 870\,K$ with parallel 500 eV Ar^+ sputtering for 0.5 hour after which the GaPAs layer showed a high-energy electron emission diffraction (RHEED) 2×2 reconstruction. Auger electron spectroscopy confirmed that after this cleaning procedure no oxygen or carbon contaminations were present. Epitaxial growth was verified by RHEED.

For our studies of RT magnetotransport across silicon TB's and voltage-regulated AF coupling, we utilized ballistic electron magnetic microscopy (BEMM). This non-destroying method with the nanometer resolution was adopted earlier for studies of spin-dependent magnetocurrent (MC) in spin valves.[13,14] In BEMM experiments, a first magnetic layer serves as a spin-polarizer and a second one as an analyzer of magnetization alignment. Ballistic hot electrons are injected across a vacuum tunnel barrier, which prevents from leakage currents and, thus, permits RT studies. The energy filtering by a Schottky barrier formed close to n-doped GaAs substrate enables to separate the tunneling current I_T from the ballistic collector current I_c. This affords a possibility to utilize tunneling currents for manipulating magnetization alignment and collector currents for detection of magnetization alignment.

A detailed description of the BEMM experimental set-up is presented in Ref. 14. The collector current I_c versus biasing voltage U_{bias} dependence taken at RT is demonstrated in Fig. 1. It is seen that for negative U_{bias} I_c increases upon overcoming a highly resistive Schottky barrier at the Fe/GaPAs interface. For negative biasing voltages exceeding 1 V, the collector current becomes dependent on the in-plane magnetic field H and reaches approximately 140 fA and 40 fA for H = 1 kOe and H = 0, accordingly. Thus, we established RT MC in AF-coupled tunneling structures based on Si. The schematic diagram of the experimental set-up is presented in the inset in Fig. 1.

In order to test whether the magnetocurrent really reflects changes in magnetization alignment, we performed comparative studies of magnetotransport and magnetic properties of our Fe/Si/Fe structures. In Fig. 2, we present MC and magneto-optical Kerr effect (MOKE) hysteresis data

a)Author to whom correspondence should be addressed. Electronic mail: rashid.gareev@physik.uni-regensburg.de.

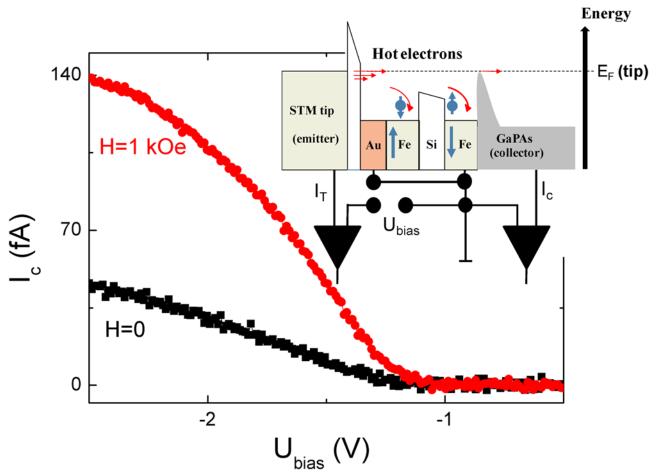

FIG. 1. (Color online) The collector current I_c versus biasing voltage U_{bias} taken in the remanent state (H = 0: squares) and above the saturation field in the parallel alignment (H = 1 kOe: circles) applied along easy axis [110] direction. The inset demonstrates the schematic diagram of the experimental set-up. Thin arrows illustrate the energy distribution of hot electrons. Thick arrows show directions of magnetic moments for iron layers and for spin-up and spin-down electrons. Hot electrons tunnel across a vacuum tunneling barrier in the direction from the STM tip to the sample surface. The tunneling current I_T becomes spin-polarized in the upper iron layer. Spin-down (spin-up) tunneling electrons are scattered mainly in the upper (bottom) magnetic layer, respectively, thus producing dynamic spin-transfer torques, which stabilize magnetization alignment. The collector current I_c consists of hot electrons with energies exceeding the height of Fe/GaPAs Schottky barrier.

taken for magnetic field applied along an easy axis. It is seen that RT hysteresis loops for MC correlate with the MOKE data and changes in the collector current reflect magnetization alignment. The magnetocurrent was determined from the equation: $MC = [(I_{cP} - I_{cAP})/(I_{cAP})]*100\%$, where I_{cP} and I_{cAP} are values of the collector current corresponding to a parallel (P) and an antiparallel (AP) alignment of magnetizations, accordingly. In our experiments, the collector current is higher for the P state compared to the AP state and exceeds 200% for $I_T = 30$ nA. The same sign of magnetocurrent was found for spin valves and explained by spin-filtering effects due to increased scattering for the minority-spin channel.[13–15]

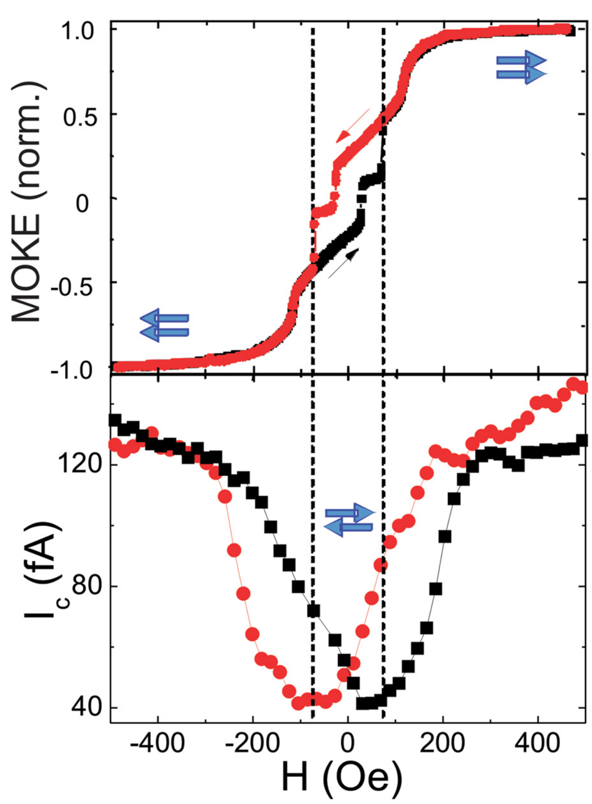

FIG. 2. (Color online) Longitudinal MOKE hysteresis and collector current I_c hysteresis taken at $U_{bias} = -2.5$ V. The in-plane magnetic field is aligned along the easy-axis [110] direction. The I_c(H) hysteresis loops are averaged over 20 cycles. Thin arrows indicate the sweep direction of the magnetic field, and thick arrows show magnetization alignment.

Next, we studied MC for different values of I_c. The increase of the saturation field H_{sat} with the tunneling current I_T (Fig. 3) upon reorientation of magnetizations between AP and P states indicates an enhancement of AF coupling by increasing I_T. Actually, as it is shown in Fig. 3, the saturation field increases from $H_{sat} \sim 300$ Oe to $H_{sat} \sim 900$ Oe upon rising of I_T from 30 nA to 50 nA. For $I_T = 60$ nA, magnetic field H = 1000 Oe is even not sufficient to switch magnetization from the AP state. For $I_T = 30$ nA and below, the tunneling current does not influence H_{sat} and AF coupling, accordingly. We determined the strength of AF coupling by fitting MOKE hysteresis curves as described elsewhere[7] and found $/J_1/\sim 35\ \mu J/m^2$ in this regime. For higher I_T, the H_{sat} increases, and transition from AP to P state becomes sharply pronounced. Taking into account that the bilinear coupling term J_1 is proportional to H_{sat},[16] we estimated that AF coupling reaches $/J_1/\sim 110\ \mu J/m^2$ ($I_T = 50$ nA) and, finally, $/J_1/$is exceeding $120\ \mu J/m^2$ for $I_T = 60$ nA. Thus, by increasing twice the tunneling current the AF coupling strength increases by a factor of three at least. It is interesting that that for $I_T = 40$ nA the collector current shows a hysteretic behavior probably due to formation of a multi-domain structure. Oscillations of the collector current in the magnetic field (Fig. 3) could be related to RT charging effects[17] upon resonant tunneling across nanometer-scaled impurities. A detailed study of charging effects is in progress and out of scope of this report.

We explain our experimental results as follows. Tunneling current I_T becomes highly spin-polarized in the upper iron layer (see the inset in Fig. 1) due to different spin-attenuation lengths for majority and minority hot-electron spins. Actually, the spin-attenuation length for the hot-electron minority spins in transition metal ferromagnets is near or below 1 nm.[13–15] For majority spins, the spin-attenuation lengths are several times bigger, and hence, they propagate across the 3 nm-thick iron mainly in the ballistic regime. Hot electrons possess energies above 2 eV and the majority spins are not substantially affected by the Si tunneling barrier (barrier height below 1 eV (Ref. 8)). In contrast, minority electrons are strongly scattered in the upper iron layer and by the Si tunneling barrier as well. Thus, two spin channels become effectively separated by the Si tunneling barrier. For the AP state, the spin-down electrons are strongly scattered in the upper iron layer and the spin-up electrons in the bottom one. In the bottom layer, tunneling electrons are filtered by the Schottky barrier, and only a small portion of carriers, mainly ballistic, reach finally the collector. In the P state, the majority spins are practically not scattered, and thus, the collector current reaches its maximum. This explains MC observed in our experiments.

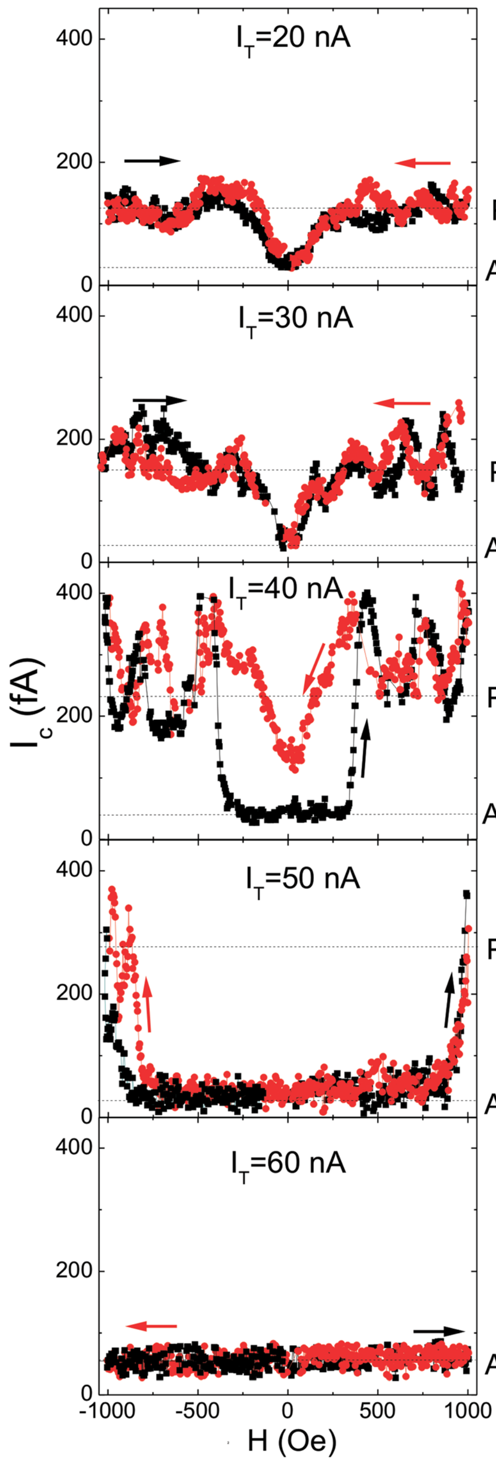

FIG. 3. (Color online) Single-cycle collector current I_c versus magnetic field aligned along [110] easy axis for different values of the tunneling current I_T measured at $U_{bias} = -2.5$ V. The squares and circles correspond to positive and negative sweep directions of magnetic field indicated by arrows, correspondingly. Parallel and antiparallel magnetization alignment is marked as P and AP, accordingly.

We connect the enhancement of AF coupling with dynamic local spin torques exerted by voltage-assisted tunneling currents. For hot-electron tunneling currents, the current density j becomes sufficient for producing substantial local dynamic spin-transfer torques. In the AP state, the spin-polarized majority (minority) electrons exert dynamic torques in the bottom (upper) iron layer (see the inset in Fig. 1). These dynamic spin torques produce an additional pinning of iron layers, which can lead to the switching of magnetization instead of the coherent rotation as observed in our experiments for I_T above 30 nA. Assuming that tunneling electrons flow from the last atom of the tip and spin-up electrons (one half of tunneling current) reach the bottom iron layer in the ballistic regime, we obtain for $I_T \sim 50$ nA that current densities are exceeding 10^7 A/cm^2. These j values, as shown for nanopillars with synthetic AF free layers,[18] are sufficient for switching of magnetization. Charging effects in magnetic tunnel junctions can also enhance spin torques compared to metallic multilayers.[19] In the presence of biasing voltage, dynamic spin torques favor stabilization of P or AP alignment depending on the direction of the tunneling current as confirmed earlier by dynamic stability diagram for spin-valves in the non-precessional regime.[20] In our experiments, dynamic spin torques favor AP alignment of magnetizations. Finally, for comparable dynamic and equilibrium spin torques, an increased AF coupling assisted by tunneling spin-polarized currents becomes detectable.

Concluding, we found RT ballistic magnetocurrent in AF-coupled Fe/Si/Fe structures. The hot-electron collector current reflects alignment of magnetizations, and the magnetocurrent exceeds 200%. The saturation magnetic field corresponding to the collector current in the parallel alignment of magnetizations increases with the tunneling current, thus demonstrating stabilization of the antiparallel alignment and the increase of AF coupling. We connect the experimentally established enhancement of AF coupling with local dynamic spin torques mediated by voltage-driven spin-polarized tunneling electrons.

This work is supported by the Project DFG 9209379.

[1] P. Grünberg, R. Schreiber, Y. Pang, M. B. Brodsky, and H. Sowers, Phys. Rev. Lett. 57, 2442 (1986).
[2] M. D. Stiles, in *Ultrathin Magnetic Structures III*, edited by B. Heinrich and J. A. C. Bland, (Springer, Berlin, 2004).
[3] G. Binasch, P. Grünberg, F. Saurenbach, and W. Zinn, Phys. Rev. B 39, 4828 (1989).
[4] J. C. Slonczewski, Phys. Rev. B 39, 6995 (1989).
[5] J. Sun, D. C. Ralph, J. Magn. Magn. Mater. 320, 1227 (2008).
[6] J. Faure-Vincent, C. Tiusan, C. Bellouard, E. Popova, M. Hehn, F. Montaigne, and A. Schuhl, Phys. Rev. Lett. 89, 107206 (2002).
[7] R. R. Gareev, D. E. Bürgler, M. Buchmeier, R. Schreiber, and P. Grünberg, J. Magn. Magn. Mater. 240, 235 (2002).
[8] R. R. Gareev, L. L. Pohlmann, S. Stein, D. E. Bürgler, P. A. Grünberg, and M. Siegel, J. Appl. Phys. 93, 8038 (2003).
[9] J. C. Slonczewski, J. Z. Sun, J. Magn. Magn. Mater. 310, 169 (2007).
[10] I. Appelbaum, B. Huang, and D. J. Monsma, Nature (London) 447, 295 (2007).
[11] M. Ye. Zhuravlev, E. Y. Tsymbal, and A. V. Vedyayev, Phys. Rev. Lett. 94, 026806 (2005).
[12] R. R. Gareev, M. Weides, R. Schreiber, and U. Poppe, Appl. Phys. Lett. 88, 172105 (2006).
[13] E. Heindl, J. Vancea, and C. H. Back, Phys. Rev. B 75, 073307 (2007).
[14] E. Heindl, C. Kefes, M. Soda, J. Vancea, and C. H. Back, J. Magn. Magn. Mater. 321, 3693 (2009).
[15] T. Banerjee, J. C. Lodder, and R. Jansen, Phys. Rev. B 76, 140407 (2007).
[16] H. Yanagihara, Y. Toyoda, and E. Kita, J. Phys. D: Appl. Phys. 44, 064011 (2011).
[17] H. Graf, J. Vancea, and H. Hoffmann, Appl. Phys. Lett. 80, 1264 (2002).
[18] T. Ochiai, Y. Jiang, A. Hirohata, N. Tezuka, S. Sugimoto, and K. Inomata, Appl. Phys. Lett. 86, 242506 (2005).
[19] Z. F. Lin, S. T. Chui, and L. B. Hu, Phys. Lett. A 332, 115 (2004).
[20] S. I. Kiselev, J. C. Sankey, I. N. Krivorotov, N. C. Emley, R. J. Schoelkopf, R. A. Buhrman, and D. C. Ralph, Nature (London) 425, 380 (2003).